MATHEMATICAL MODELLING AND SIMULATION OF DROPWISE CONDENSATION AND INCLINED SURFACES EXPOSED TO VAPOR FLUX

Nirmal Kumar Battoo
Department of Mechanical Engineering
Indian Institute of Technology Kanpur
Kanpur 208016, India
battoo@iitk.ac.in

Basant Singh Sikarwar
Department of Mechanical Engineering
Indian Institute of Technology Kanpur
Kanpur 208016, India
sikarwar@iitk.ac.in

Sameer Khandekar
Department of Mechanical Engineering
Indian Institute of Technology Kanpur
Kanpur 208016, India
samkhan@iitk.ac.in

K. Muralidhar
Department of Mechanical Engineering
Indian Institute of Technology Kanpur
Kanpur 208016, India
kmurli@iitk.ac.in

ABSTRACT

Computer simulation of dropwise condensation on a substrate, having randomly spaced nucleation sites, is described. A numerical model is presented for simulation of dropwise condensation on flat and inclined surfaces exposed to a vapor flux. The model incorporates the effect of contact angle, inclination, contact angle hysteresis and saturation temperature at which the condensation is carried out. Simulation accounts for direct condensation growth, coalescence, fall-off and renucleation of droplets. Numerical computations are conducted for various contact angles and substrate inclination angle as a parameter. Drop size distributions and spatial patterns of condensation are presented. The simulation results are satisfactorily compared with experimental data.

NOMENCLATURE

A	Area of cross section (m^2)
α	Void fraction (-)
T_w	Temperature of the solid wall (K)
T_{sat}	Saturation temperature of the condensate (K)
h_{lv}	Latent heat of vaporization of the liquid (kJ/kg)
h_l	Interfacial heat transfer coefficient (W/m^2-K)
K_c	Condensate thermal conductivity (W/m-K)
r_{min}	Minimum Radius of droplet (m)
r_{max}	Radius of the departing droplet (m)
r_b	Base radius of the droplet (m)
r_{crit}	Critical radius of droplet on an inclined substrate (m)
r	Radius of droplet (m)
A_{lv}	Area of liquid vapor interface (m^2)
A_{sl}	Area of solid liquid interface (m^2)
V_{sc}	Volume of the spherical cap (m^3)
ΔT_{cond}	Temperature drop due to conduction (K)
ΔT_{curv}	Temperature drop due to curvature resistance (K)
ΔT_{int}	Temperature drop due to interfacial heat and mass transfer (K)
ΔT_t	Total temperature drop (K)
q	Heat flux (W/m^2)
M	Total number of nucleation sites
$\dot{m}$	Vapor mass flux (kg/s)
$\overline{R}$	Universal gas constant (J/kmol·K)
$\overline{M}$	Molecular weight of the condensing liquid (kg/kmol)
Δt	Time step (s)
h	Height of center of mass of the droplet (m)
$F_r\|\|$, $F_r\perp$	Parallel and perpendicular retention force to the substrate (N)
$F_g\|\|$, $F_g\perp$	Parallel and perpendicular gravity force to the substrate (N)
F_s	Viscous force on the moving droplet (N)
U	Velocity of the moving droplet (m/s)
U_{cyrr}, U_{prev}	Velocities of the droplet at current and previous time step (m/s)
a_d	Acceleration of the moving droplet (m^2/s)
σ	Surface tension (N/m)
v_l	Specific volume of liquid at the saturation temperature (m^3/kg)
v_v	Specific volume of vapor at the saturation temperature (m^3/kg)
$\hat{\sigma}$	Accommodation coefficient (-)
θ_{avg}	Average contact angle (rad)
α_i	Inclination angle (rad)
ρ_l, ρ_v	Density of condensate and vapor (kg/m^3)
θ_{adv}	Advancing angle (rad)
θ_{rcd}	Receding angle (rad)
ϕ	Azimuthal angle (rad)
η	Viscosity (Pa-s)
τ	Shear stress (N/m^2)

20th National and 9th International ISHMT-ASME Heat and Mass Transfer Conference
Edited by Kannan N. Iyer

ISBN: 978-981-08-3813-3
doi:10.3850/9789810838133_346

INDRODUCTION

Condensation is one of the major processes of heat transfer in a variety of industries. Any method or process of enhancing the condensation heat transfer coefficient would greatly reduce the pumping power and also the size of the equipment. Over the years, many experimental and theoretical research papers have reported enhancement of heat transfer by dropwise condensation and the underlying mechanism of the dropwise condensation. Although dropwise condensation has been a matter of interest for a long time but the mechanism of dropwise condensation is not fully clear yet. Two different models have been proposed for the mechanism. The first model is based on the premise that droplet formation is a heterogeneous nucleation process. Droplet embryos are postulated to form and grow at nucleation sites, while the portion of the surface between the growing droplets remains dry. This type of model was first proposed by Eucken [1]. Some experimental results do support this contention that the microscopic droplets are nucleated at active nucleation sites on the cooled surface. In the second dropwise condensation model, it is postulated that condensation occurs initially in a filmwise manner, forming an extremely thin film on the solid surface. As condensation continues in time, this film ruptures and distinct droplets are formed. Condensation then continues on the surface between the droplets that form when the film ruptures. Condensate produced in these regions is drawn to adjacent drops by the action of surface tension forces. Droplets also grow by direct condensation on the droplet surfaces themselves. Glicksman and Hunt [2] simulated dropwise condensation cycle in a number of stages to achieve a large nucleation site density and the range covering the equilibrium drop size to departing drop size. The initial stage consisted nucleation site density of 10^8 sites per square cm, by taking 1000 sites on a surface of 33 x 33 μm. The area of the second stage was increased ten times and the droplets from the first stage were redistributed on this surface. In this way they repeated the simulations until they reached the departure droplet size. In this method of simulation, a high nucleation site density was archived but redistribution of the drops between two consecutive stages destroyed the natural distribution of the drops. Wu and Maam [3, 4] used the population balance method to find the drop size distribution of small drops which grow mainly by direct condensation. The authors estimated the heat transfer coefficient by considering only the conduction resistance through the drop. Abu-Orabi [5] incorporated the resistance due to heat conduction through the promoter layer, and curvature resistance into his model, because considering only conduction resistance, overestimates heat transfer. This overestimation increases as the temperature difference increases. Rose and Glicksman [6] proposed a universal form of the distribution function for large drops which grow primarily by coalescence with smaller drops, though smaller drops mainly grow by direct condensation. Gose et al. [7] carried out computer simulation on 100 x 100 grid with 200 randomly distributed nucleation sites. Burnside and Hadi [8] simulated dropwise condensation of steam from equilibrium droplet to detectable size on 240 x 240 μm surface with 60000 randomly spaced nucleation sites. Later, Vemuri and Kim [9] modelled dropwise condensation by population balance method for hemispherical drops which mainly grow by direct condensation. The important resistances to heat transfer such as conduction through the drop and vapor-liquid interface were considered in developing the model. The derivation of steady state distribution for small drops within the size range of negligible coalescence was based on the conservation of the number of drops with no accumulation. Contact angle other than 90° was not considered in this model. A population balance model at atomistic level has been proposed by Sumeet Kumar et al. [10] to predict the critical cluster size during condensation of saturated vapor on a sub-cooled surface. The model is posed in terms of three parameters, namely the diffusion constant, the residence time and applied vapor flux. The largest cluster size determined from atomistic consideration is the smallest drop size on macroscopic scale. The authors found that the largest cluster size or the smallest drop size at the macroscale is a function of surface diffusion coefficient and applied vapor mass flux. An increase in these values result in an increase of the largest cluster size. Till date a simulation of dropwise condensation from equilibrium droplet size to departing droplet size accounting for the effect of contact angle and inclination has not been reported. The present study aims to model and simulate the complete process of dropwise condensation from equilibrium droplet size up to the departing droplet size. A detailed computer simulation is carried out on a substrate with nucleation sites density of 10^9 sites per square meter for horizontal and inclined arrangements and for different fluids. Temporal and spatial drop distribution patterns and drop size distribution are obtained. Condensation experiments have been performed on chemically coated glass surface for both horizontal and inclined arrangements of substrate. Chemical coating promotes dropwise condensation by rendering the surface hydrophobic. Silanised glass surfaces have been prepared. The static contact angle of deionized water has been measured. The drop size distribution images of condensation are recorded with a CCD camera. The simulations are compared with the experimental data.

MODEL DEVELOPMENT

Following Vemuri and Kim [9], a population balance concept has been used to predict the number of small drops within the size range of negligible coalescence. The smallest radius of droplet by thermodynamic considerations that can grow for a given wall sub-cooling is

$$r_{\min} = \frac{2\sigma v_l T_w}{h_{lv}[T_s - T_w]} \tag{1}$$

The pendant drop underneath a flat horizontal substrate is shown in Figure 1. The drop is considered as a portion of a sphere making a contact angle α = (180-θ). From the drop geometry, the drop volume *V*, area of liquid-vapor interface A_{lv}, area of solid-liquid interface A_{sl} are expressed by the following equations:

$$V = \frac{\pi r^3}{3}\left(2 + 3\cos\theta - \cos^3\theta\right) \tag{2}$$

$$A_{lv} = 2\pi \cdot r^2\left(1 + \cos\theta\right) \tag{3}$$

$$A_{sl} = 2\pi \cdot r^2\left(1 - \cos^2\theta\right) \tag{4}$$

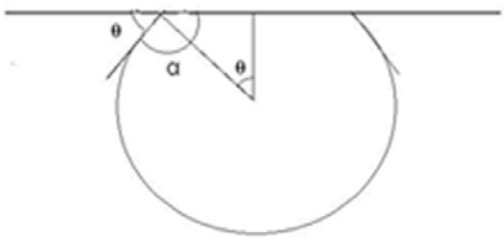

Figure 1. Drop underneath a horizontal substrate making a contact angle α.

The maximum drop diameter is calculated from balancing the surface tension force to the weight of the droplet as:

$$r_{\max} = \sin\theta \cdot \sqrt{\frac{6\sigma}{g(\rho_l - \rho_v) \times (2 + 3\cos\theta - \cos^3\theta)}} \quad (5)$$

The drops in temperature for a droplet due to resistances to heat transfer are determined as given below.

1. The drop in temperature due to the conduction heat transfer through a hemispherical droplet is given by Orabi [5]

$$\Delta T_{cond} = (q \cdot r) / \left(4\pi \cdot r^2 \cdot k_c\right) \quad (6)$$

here q is heat transfer from a droplet. When contact angle is taken into account in Eq. 6 it is modified as:

$$\Delta T_{cond} = (q \cdot r) / \left(4\pi \cdot r^2 \cdot k_c \left(1 + \cos\theta\right)\right) \quad (7)$$

2. Temperature drop due to interfacial heat transfer resistance is given by:

$$\Delta T_{\text{int}} = q / \left(2\pi \cdot r^2 \cdot h_i \left(1 + \cos\theta\right)\right) \quad (8)$$

Here, interfacial heat transfer coefficient h_i comes from the kinetic theory of gases [1], and is expressed as:

$$h_i = \left(\frac{2\hat{\sigma}}{2 - \hat{\sigma}}\right)\left(\frac{h_{lv}^{\ 2}}{T_s \cdot v_{lv}}\right)\left(\frac{\overline{M}}{2\pi \cdot \overline{R} T_s}\right)^{1/2} \quad (9)$$

where, $\hat{\sigma}$ is accommodation coefficient, which defines the fraction of the striking molecules that actually get condensed on the substrate.

3. Curvature of the liquid vapor interface results in an equilibrium saturation temperature which is lower than the saturation temperature at a planar interface. The difference in the equilibrium temperature of saturated vapor at a planar interface and at a curved interface is given by:

$$\Delta T_{curv} = \frac{2v_l \cdot \sigma \cdot T_w}{h_{lv} \cdot r} = \frac{r_{\min}\left(T_s - T_w\right)}{r} \quad (10)$$

The total temperature drop from vapor at its saturation temperature to the solid condensing surface is the sum of the temperature differences due to curvature, interfacial heat and mass transfer and conduction:

$$\Delta T_t = \Delta T_{cond} + \Delta T_{\text{int}} + \Delta T_{curv} \quad (11)$$

The net heat transfer through a single drop is determined as

$$q = \pi r^2 \cdot \rho_l \cdot h_{lv}\left(2 + 3\cos\theta - \cos^3\theta\right)\frac{dr}{dt} \quad (12)$$

On substitution of Eqs. 7, 8, 10 and Eq. 11, we get direct condensation growth rate for a droplet.

$$\frac{dr}{dt} = \frac{4\Delta T_t}{\rho_l \cdot h_{lv}}\left[\frac{\left(1 - \frac{r_{\min}}{r}\right)}{\frac{2}{h_i} + \frac{r}{k_c}}\right]\left(\frac{(1 + \cos\theta)}{(2 + 3\cos\theta - \cos^3\theta)}\right) \quad (13)$$

Eq. 13 represents the growth rate of the droplet when condensing vapor is stagnant. When the vapor is not stagnant, rather it is fed as a directed mass flux, an additional term will be added to Eq. 13; that term is calculated as given below:

$$\dot{m} A_{sl} = \rho_l \left(dV / dt\right) \quad (14)$$

where $\dot{m}$ is mass flux per unit area of the substrate per unit time. After rearranging Eq. 14 we get,

$$\frac{dr}{dt} = \frac{\dot{m}\left(1 - \cos^2\theta\right)}{\rho_l\left(2 + 3\cos\theta - \cos^3\theta\right)} \quad (15)$$

The general equation for growth of a droplet due to direct condensation on it is obtained as:

$$\frac{dr}{dt} = \frac{4\Delta T_t}{\rho_l \cdot h_{lv}}\left[\frac{\left(1 - \frac{r_{\min}}{r}\right)}{\frac{2}{h_i} + \frac{r}{k_c}}\right]\left(\frac{(1 + \cos\theta)}{(2 + 3\cos\theta - \cos^3\theta)} + \frac{2\dot{m}\left(1 - \cos^2\theta\right)}{\rho_l\left(2 + 3\cos\theta - \cos^3\theta\right)}\right) \quad (16)$$

This equation has been integrated to determine the growth of droplet due to direct condensation. Along with the growth loop, a coalescence loop is applied, in which, as soon as two (or three or four) droplets touch each other, they are removed and a drop with equivalent volume is substituted at the center of mass of the coalescing droplets. In each time step, the nucleation sites which are covered by drops are made as hidden sites. In this way the droplets are allowed to grow to the critical stage, where gravity force exceeds the surface tension. At this instant, fall-off takes place and the particular drop is removed. All hidden sites underneath this drop become active once again and supplied with the thermodynamically sustainable minimum radius. The cycle begins again and is repeated till a dynamic steady-state is reached.

Condensation underneath an inclined substrate

Inclining the substrate causes imbalance in the forces and results in drop deformation to achieve a force balance. Gravity force will cause the droplet to slide on the substrate when it exceeds the retention force due to surface tension. Deformation of drop causes contact angle hysteresis. Here, contact angle hysteresis is taken into account by assuming the contact angle to vary linearly from advancing to the receding angle with respect to azimuthal angle along the contact line. The base of the droplet is assumed to be circular. Figure 2 shows a deformed pendant droplet underneath an inclined substrate. The variation of contact angle with respect to azimuthal angle along the contact line is given as:

$$\theta = \theta_{adv} + \frac{\pi - \theta_{rcd} - \theta_{adv}}{\pi}\phi \quad (17)$$

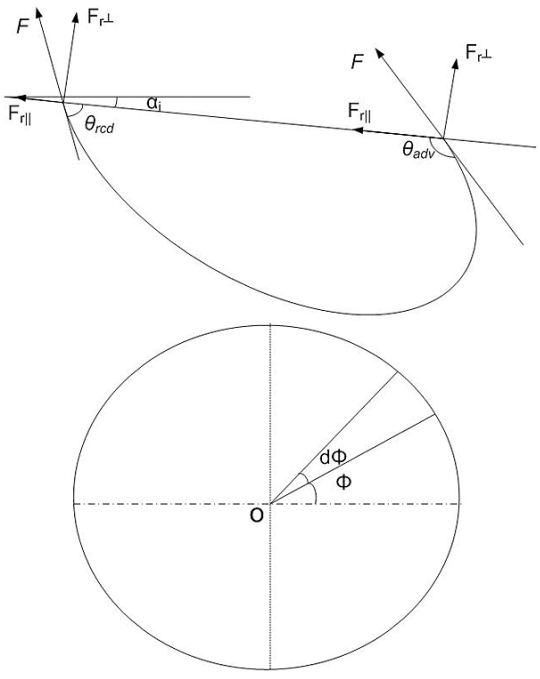

Figure 2. A deformed pendant drop underneath an inclined substrate.

The retention force parallel to the substrate due to imbalance in the surface tension force is expressed as

$$F_{r\parallel} = 2\int_0^{\pi} \sigma \cdot r_b \cdot \cos\theta \cdot \cos\phi \cdot d\phi \tag{18}$$

$$F_{r\parallel} = \sigma r_b \left[\frac{\pi}{2\pi - \theta_{rcd} - \theta_{adv}} \left\{ \sin\left(2\pi - \theta_{rcd}\right) - \sin\theta_{adv} \right\} + \frac{\pi}{\theta_{adv} + \theta_{rcd}} \left\{ \sin\theta_{rcd} + \sin\theta_{adv} \right\} \right] \tag{19}$$

Spherical cap approximation

The main problem in modelling dropwise condensation is deformed shape of the droplet due to the inclination. To overcome this difficulty, a spherical cap approximation is used. The drop is assumed to be a segment of a sphere with the contact angle θ_{av} The volume of the spherical cap V_{sc} is determined by

$$V_{sc} = \frac{\pi r_b^3 \left(2 - 3\cos\theta_{av} + \cos^3\theta_{av}\right)}{3\sin^3\theta_{av}} \tag{20}$$

$$\theta_{av} = \frac{\theta_{rcd} + \theta_{adv}}{2} \tag{21}$$

Calculation of critical radius of droplet

The gravity force parallel and perpendicular to the substrate are expressed as

$$F_{g\parallel} = \frac{\pi r_b^3 \left(2 - 3\cos\theta_{av} + \cos^3\theta_{av}\right)}{3\sin^3\theta_{av}} \rho g \sin\alpha_i \tag{22}$$

$$F_{g\perp} = \frac{\pi r_b^3 \left(2 - 3\cos\theta_{av} + \cos^3\theta_{av}\right)}{3\sin^3\theta_{av}} \rho g \cos\alpha_i \tag{23}$$

The critical radius of droplet on inclined substrate is calculated by balancing the forces parallel to the substrate due to surface tension and gravity. The critical radius is expressed as

$$r_{crit}^2 = \left[\left(\frac{3\sigma \sin\theta_{av}}{\pi\left(2 - 3\cos\theta_{av} + \cos^3\theta_{av}\right)\rho g \sin\alpha_i} \right) \cdot \left(\frac{\pi}{2\pi - \theta_{rcd} - \theta adv} \left\{ \sin\left(2\pi - \theta_{rcd}\right) - \sin\theta_{adv} \right\} + \frac{\pi}{\theta_{adv} + \theta_{rcd}} \left\{ \sin\theta_{rcd} + \sin\theta_{adv} \right\} \right) \right] \tag{24}$$

The force due to surface tension perpendicular to the inclined substrate is determined by

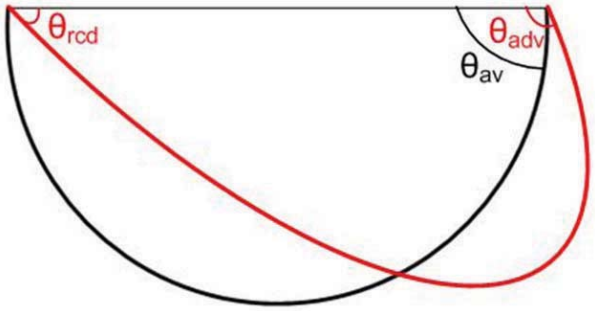

Figure 3. Spherical cap approximation of deformed droplet underneath inclined surface.

$$F_{r\perp} = 2\int_0^{\pi} \sigma \cdot r_b \cdot \sin\theta \cdot d\phi \tag{25}$$

$$F_{r\perp} = 2\sigma \cdot r_b \left(\frac{\pi}{\pi - \theta_{rcd} - \theta_{adv}} \right) \left(\cos\theta_{rcd} + \cos\theta_{adv} \right) \tag{26}$$

The maximum radius of a stable droplet obtained by balancing the forces perpendicular to the substrate is

$$r_{\max} = \sqrt{\frac{6\sigma \cdot \sin\theta_{av} \cdot \left(\cos\theta_{rcd} + \cos\theta_{adv}\right)}{\rho \cdot g \cdot \cos\alpha_i \left(2 - 3\cos\theta_{av} + \cos^3\theta_{av}\right)\left(\pi - \theta_{rcd} - \theta_{adv}\right)}} \tag{27}$$

Acceleration and velocity of droplet

After achieving the critical volume, further growth will cause commencement of sliding; the sliding drop will accelerate on the surface and collide with the droplets ahead. This results in further coalescence and acceleration of the droplet. The acceleration of the droplet is calculated by Newton's second law of motion. The forces on the sliding droplet parallel to the substrate are:

1. Gravity force F_g
2. Force due to shear at the wall F_s
3. Retention force due to surface tension $F_{r||}$

Many researchers dealt with the problem of motion of droplet on an inclined substrate. Sakai et al.[15] have shown that velocity varies linearly inside a moving droplet; Following [15] a linear velocity distribution is assumed inside the moving droplet, the maximum velocity is taken at the center of mass of the droplet. The velocity gradient and shear stress are calculated as

$$\frac{du}{dy} = \frac{U}{h} \tag{28}$$

$$\tau = \mu_l \frac{du}{dy} = \mu_l \frac{U}{h} \tag{29}$$

From force balance, the acceleration and velocity of the droplet is thus calculated:

$$a = \frac{F_{g\parallel} - F_s - F_{r\parallel}}{m} \tag{30}$$

$$U_{curr} = U_{prev} + a \cdot dt \tag{31}$$

RESULTS AND DISCUSSIONS

Numerical computations are conducted for 10^8-10^9 sites per m^2 nucleation site density for various contact angles. Figure 4 and Figure 5 show the mechanism of nucleation, coalescence, fall-off, commencement of sliding, sweeping effect of sliding droplet and renucleation.

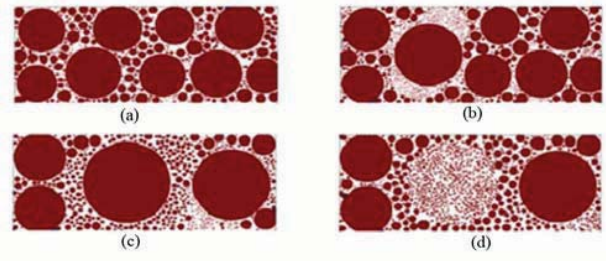

Figure 4. Coalescence, falloff and renucleation of droplets on horizontal substrate. (a) and (b) show the coalescence, (c) and (d) show falloff and re-nucleation.

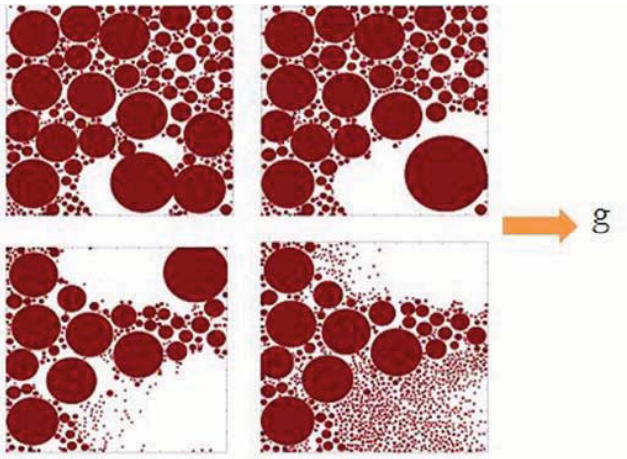

Figure 5. Sliding falloff and renucleation of drops of water in dropwise condensation on a 10^{o} inclined substrate.

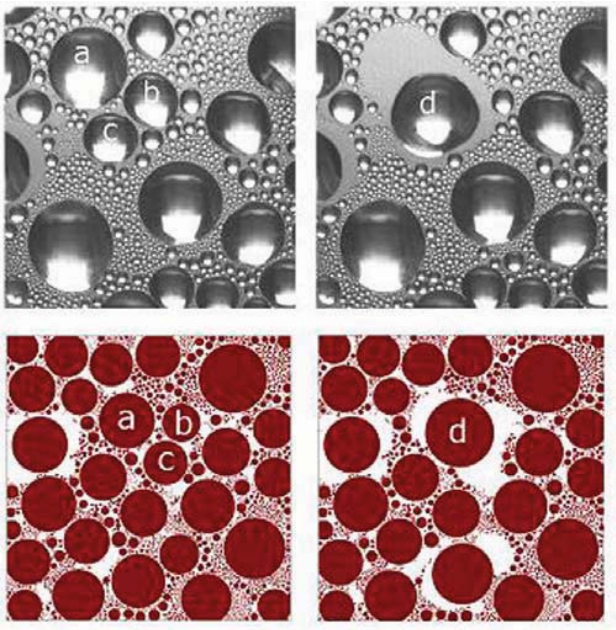

Figure 6. Common centers after Coalescence in experiments and simulation.

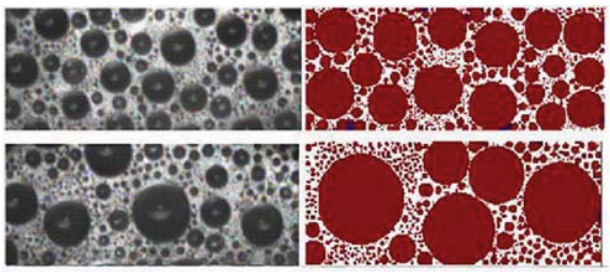

Figure 7. Experimental [16] and simulated drop distribution pattern on a 25 *mm* x 10 *mm* horizontal substrate at 14 and 28 minutes respectively.

Figure 6 shows the phenomena of coalescence observed in experimentation and as captured by simulation. It is clear that after coalescence, the coalescing droplets get positioned at the center of mass Figure 7 shows the experimental [16] and

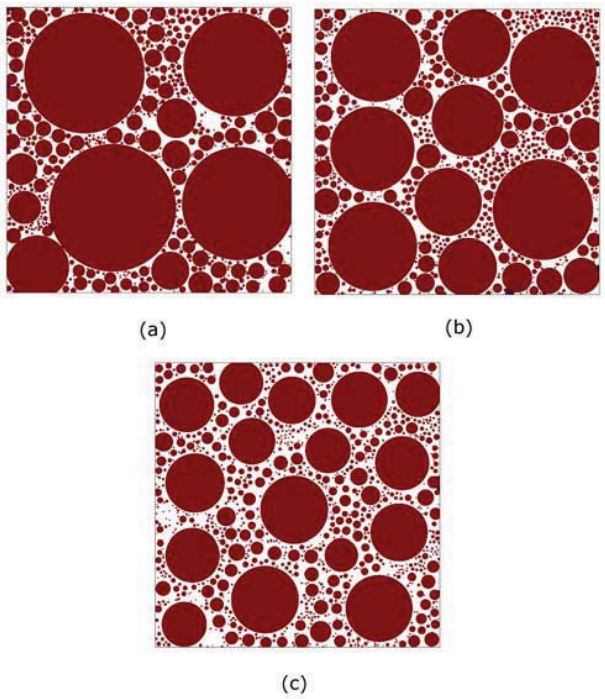

Figure 8. Spatial drop distribution just before fall-off on a substrate of area 20 x 20 mm^2 for different contact angles (a) 90^{o} (b) 105^{o} (c) 120^{o}.

simulated spatial drop distribution. The model is seen to capture the inherent mechanism of dropwise condensation satisfactorily. The effect of contact angle is explored in table 2; it shows the percentage area coverage for different contact angles. Area of coverage by drops first increases as droplets grow and achieves a steady value after many coalescence and fall-off cycles. Large local fluctuations in area of coverage show the instants where departure of droplet has just taken place. As contact angle increases the average area of coverage decreases. Figure 8 shows the spatial drop distribution just before fall-off on a substrate of 20×20 mm^2 area for different contact angles. Varying the contact angle changes the drop distribution; higher the contact angle, lower the departing droplet size and large number density of small droplets.

Table 1 shows that the average area of coverage decreases with increasing the inclination angle. Inclining the substrate increases smaller drops. An increase in contact angle in dropwise condensation on horizontal plate results in earlier fall-off has been shown Figure 9. Figure 10 shows the spatial distribution of droplets underneath a horizontal substrate for liquid sodium and water. Owing to the higher surface tension of liquid sodium the departing droplet size is large as compared to water. Figure 11 represents the effect of liquid-solid combination on number density distribution. In case of liquid metal a large number of small drops are present on the substrate whereas the number density of small drops in water is less. The variation of critical angle of inclination for commencement of sliding with respect to the radius of the droplet for a specified advancing and receding angles and for various liquid metals is shown in Figure 12. Increasing the radius decreases the critical angle. Critical angle of inclination also depends on the surface tension of the liquid; larger surface tension fluids have a large critical inclination angle. The effect of contact angle hysteresis on the critical angle of inclination is demonstrated by Figure 13. Figures 11-13 show the effect of thermo-physical properties of the solid-liquid pair in dropwise condensation.

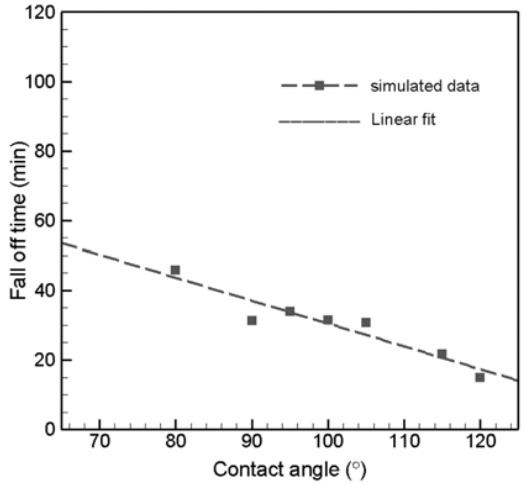

Figure 9. Effect of contact angle on fall-off time.

.

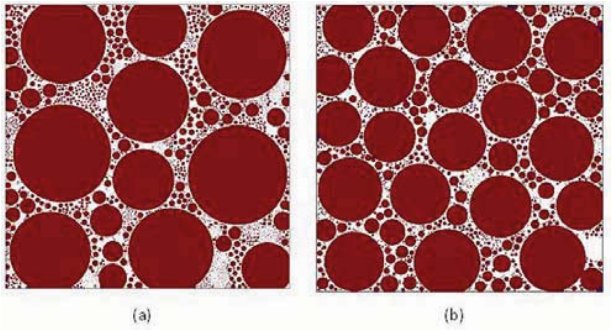

Figure 10. Spatial drop distributions for dropwise condensation underneath horizontal stainless steel substrate for (a) liquid sodium (b) water.

Table 1: Average area of coverage with respect to inclination angle condensation underneath an inclined substrate

Inclination angle	Average area of coverage
0°	76.1%
5°	71.2%
10°	67.4%

Table 2: Area of coverage for different contact angles in dropwise condensation of water without applied mass flux

Contact angle	Average area of coverage
90°	73.3%
105°	67.2%
120°	52.4%

As the hysteresis is reduced the critical angle of inclination reduces. Figure 14 shows the temporal variation of drop size distribution for 10^9 sites/m^2 nucleation sites density on a substrate of 10 $mm \times 10$ mm area for water. Using regression, the drop size distribution was seen to obey a power law:

$$\ln N = r^{-1.189} - 1.397 \qquad (32)$$

The effect of saturation temperature on dropwise condensation is explained in Figure 15. The interfacial heat transfer coefficient h_i is a function of temperature and pressure; as pressure increases, h_i, and hence rate of growth of droplet, increases. Increasing the saturation temperature results in earlier fall-off.

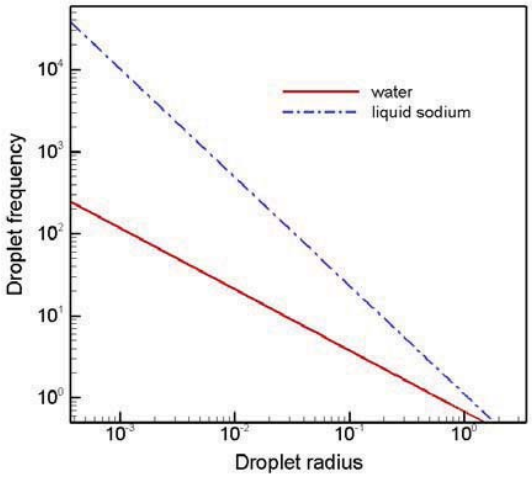

Figure 11. Effect of thermo-physical properties of liquid-solid pair on drop size distribution.

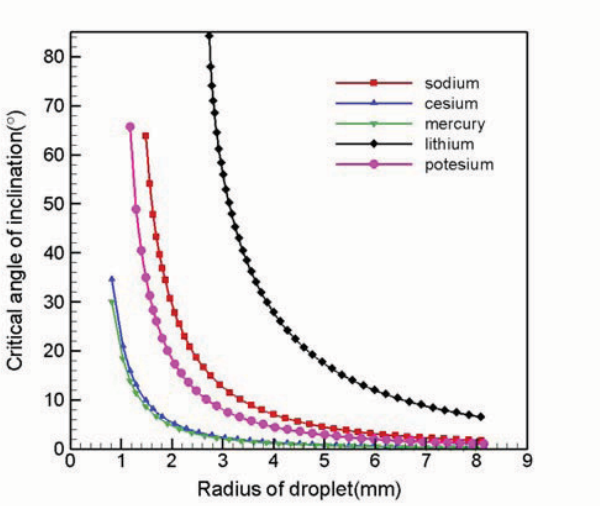

Figure 12. Variation of critical angle of inclination for commencement of sliding for different fluids with respect to critical radius of droplet for a given shape advancing angle = 120° and receding angle = 50°.

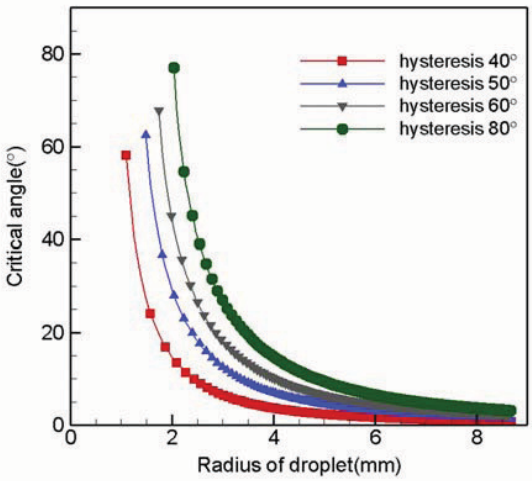

Figure 13. Variation of critical angle of inclination for commencement of sliding of water droplet, with respect to critical radius of droplet, at different contact angle hysteresis.

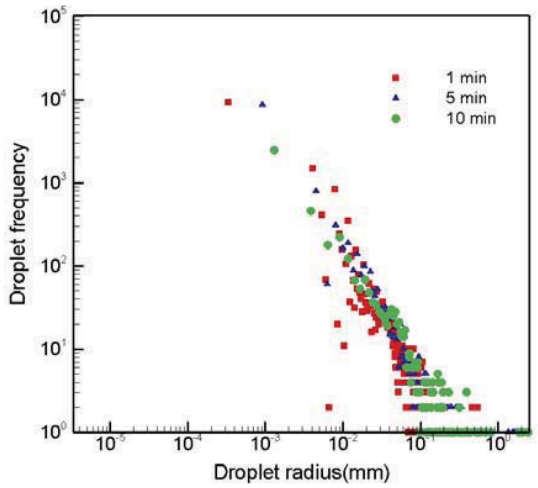

Figure 14. Temporal variation of drop size distribution.

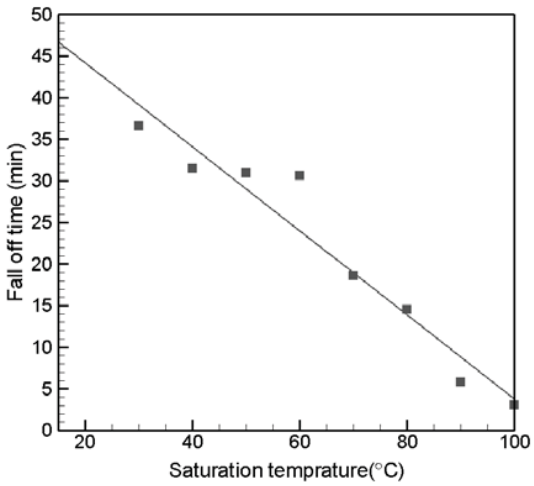

Figure 15. Variation in drop departure time with respect to saturation.

CONCLUSIONS

A detailed simulation of dropwise condensation underneath horizontal and inclined substrates has been carried out for various contact and inclination angles. The effect of various parameters such as contact angle, contact angle hysteresis, inclination angle, and saturation temperature is investigated. Condensation experiments have been carried out on chemically coated glass substrate to understand the mechanism of dropwise condensation. The following conclusions have been arrived at in the present study:

1. The mathematical model captures the process of dropwise condensation satisfactorily.
2. Area fraction covered by the drops increases as drops grow and achieves a steady state after many cycles of coalescence and fall-off.
3. The effect of contact angle and inclination on the area coverage to reduce the fraction of area covered by drops. Increase in contact angle results in earlier fall-off.
4. Inclining the substrate results in larger number of small drops and hence in higher heat transfer coefficient as resistance to heat transfer is less in smaller drops as compared to larger drops.
5. At higher saturation temperature, the rate of growth of droplet is higher; the reason behind this is the interfacial heat transfer coefficient. It increases as temperature and pressure increase, hence, at higher saturation temperature early fall-off is observed.
6. The critical radius of droplet at which commencement of sliding takes place is a function of thermo-physical properties of the fluid, inclination angle of the substrate and contact angle hysteresis. Fluids with higher surface tension show larger critical radius. Reduction in contact angle hysteresis reduces the critical radius of the droplet at fall-off for a given angle of inclination.

ACKNOWLEDGEMENT

Financial assistance by the Board of Research in Nuclear Sciences, Mumbai under the project BRNS/ME/20050106 is gratefully acknowledged.

REFERENCES

[1] Carey V. P., *Liquid-vapor phase-change phenomena*, Hemisphere Publishing Corp., New York, 1992.

[2] R. L. Glicksman, W. A. Hunt, Numerical simulation of dropwise condensation, *Int. J. Heat Mass Trans*., vol. 15 (1972), pp. 2251-2269.

[3] W. H. Wu, J. R. Maa, On the heat transfer in dropwise condensation, *Chem. Eng. J*., vol. 12 (1976), pp. 225-231.

[4] J. R. Maa, Drop size-distribution and heat flux of drop-wise condensation, Chem. Eng. J., vol. 16 (1978), pp. 171-176.

[5] M. Abu-Orabi, Modeling of heat transfer in dropwise condensation, *Int. J. Heat Mass Trans.*, vol. 41 (1998), pp. 81-87.

[6] J. W. Rose, L.R. Glicksman, Dropwise condensation the distribution of drop sizes, *Int. J. Heat Mass Trans.,* vol. 16 (1973), pp. 411-425.

[7] E. Gose, A. N. Mucciordi, and E. Baer, Model for dropwise condensation on randomly distributed sites, *Int. J. Heat Mass Trans*., vol. 10 (1967), pp. 15-22.

[8] B. M. Burnside, H.A. Hadi, Digital computer simulation of dropwise condensation from equillibrium droplet to detectable size, *Int. J. of Heat Mass Trans.,* vol. 42 (1999), pp. 3137-3146.

[9] S. Vemuri, K. J. Kim, An experimental and theoretical study on the concept of drop wise condensation, *Int. J. of Heat Mass Trans.*, vol. 49 (2006), pp. 649-657.

[10] Sumeet Kumar, Sameer Khandekar, and K. Muralidhar, Determination of the critical cluster size during dropwise condensation by an atomistic model, manuscript under preparation (2009).

[11] E. B. Dussan V and R. T. Chow, On the ability of drops or bubbles to stick to non-horizontal surfaces of solids, *J. of Fluid Mechanics*, vol. 137 (1983), pp. 1-29.

[12] B. J. Briscoe, K. P. Galvin, The sliding of sessile and pendant droplets, The critical condition, *J. of Colloid and Interface Science* vol. 52 (1991), pp. 219-229.

[13] E. Chibowski, On some relations between advancing, receding and Youngs contact angles, *Adv. in Colloid Interface Science,* vol. 133 (2007), pp. 51-59.

[14] A. I. ElSherbini and A. M. Jacobi, Liquid drops on vertical and inclined surfaces I. An experimental study of drop geometry, *J. of Colloid Interface Science*, vol. 273 (2003), pp. 556-565.

[15] M. Sakai, A. Hashimoto, N. Yoshida, S. Suzuki, Y. Kameshima and A. Nakajima, Image analysis system for evaluating sliding behavior of a liquid droplet on a hydrophobic surface, *Rev. Scientific Instrument*, vol. 78 (2007), 045103.

[16] Agarwal Smita, Dropwise condensation on chemically modified surfaces, M. Tech. thesis, Department of Mechanical Engineering, I.I.T. Kanpur (2008).